A SEMI-ANALYTICAL MODELING OF COUPLED PIEZOELECTRIC RESONATORS BASED ON SUPPORT TRANSDUCER TOPOLOGY

Chin-Yu Chang[1], *Gayathri Pillai*[2], *and Sheng-Shian Li*[1,3]
[1]Institute of NanoEngineering and MicroSystems, National Tsing Hua University, Hsinchu, Taiwan
[2]Center for Nanoscience and Engineering, Indian Institute of Science, Bengaluru, India
[3]Department of Power Mechanical Engineering, National Tsing Hua University, Hsinchu, Taiwan

ABSTRACT

This work investigates, for the first time, an analytical model of a generic coupled piezoelectric resonator based on support transducer topology. Since a "coupled resonator" consists of multiple length extensional mode (LE) transducer arms and an isochoric bulk mode resonator, we treat each component as a distinct sub-resonator and integrate them into a multiple-port electromechanical circuit based on an array-composite concept. In this work, 2-D finite-element method (FEM) simulations are performed to compensate the uncertainty of analytical solution on the electromechanical coupling coefficient (k_t^2) caused by the elastic modulus mismatch between the single crystal silicon (SCS) passive layer and the aluminum nitride (AlN) transducer. For verification, a TPoS coupled resonator based on AlN-on-Si topology is simulated with the proposed numerical model, showing a motional resistance (R_m) prediction error less than 3.5% and 13.2% as compared with FEM and measurement results, respectively.

KEYWORDS

Support Transducer, Coupled Resonator, TPoS, Analytical Modeling

INTRODUCTION

Microelectromechanical System (MEMS) oscillator has become one of the most popular future timing solutions in the consumer electronic systems [1]. It features with high operating frequency, compact volume, great robustness, and low environmental sensitivity. The quality of the output signal in an oscillator system is represent by frequency stability. Higher quality factor (Q) and lower motional impedance (R_m) from the resonator system can leading to a good frequency stability performance [2]-[4]. Among the existing MEMS technology, capacitive resonators fabricated by single crystal silicon (SCS) have been proofed to enable adequate close to carrier phase noise performance by the high Q-factor [5]. Nonetheless, the large R_m and the demand of high dc-bias voltage for large electrostatic force cause the inconvenience for the sustaining circuit design [6]. Hence, piezoelectric resonator with low R_m from the high electromechanical coupling becomes the better solution for the oscillator system design. However, piezoelectric resonator usually suffers from low Q-factor due to the interfacial material loss from the heterogeneous layer stacking in the piezoelectric resonator. This drawback could be solved by the proposed support transducer topology.

From our previous work, support transducer topology (STT) is a proven technique to enable high Q-factor bulk mode resonator with piezoelectric transduction [7]-[9]. This topology is realized by multiple length extensional (LE) mode resonator and a bulk mode resonator (e.g., Lamé, elliptical mode), as shown in Fig 1. The LE-mode transducer arm driven the bulk mode at the center into desire mode shape efficiently by matching the resonant frequency between resonators. The energy could be conserved inside the resonator system by implementing the high Q bulk mode resonant plate which

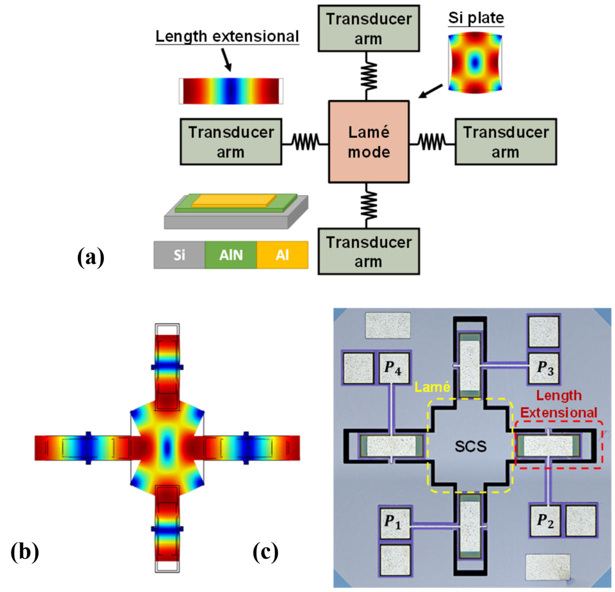

Figure 1: (a) Schematic of the support transducer topology where the transducer arms are placed around the peripheral of the resonator tank, (b) simulated mode shape of the proposed support transducer Lamé mode resonator, and (c) optical image of the fabricated device.

construct by SCS. Previous works has demonstrated that this topology could provide high Q-factor and low R_m for piezoelectric resonator which leading a better close to carrier phase noise performance [10]. Although the theoretical expression of the piezoelectric contour mode resonators has been well studied [11]-[12]. However, the analytical modeling for this unique coupled resonator system has never been reported.

In this work, the support transducer Lamé mode resonator is divided into multiple distinct sub-resonators being integrated into a multiple-port electromechanical circuit based on an array-composite concept. The mismatch of the electromechanical coupling from the theorical calculation is compensated by the use of FEM. The frequency response of the support transducer resonator is successfully predicted by the proposed analytical solution with acceptable error.

ANALYTICAL MODELING

Overview of the analytical model

Fig. 2(a) presents the schematic of the proposed analytical model where each sub-resonator is represented by a series RLC model. The overall system contains the LE-mode resonators which are actuated by piezoelectric effect from the AlN thin-film while the Lamé mode resonant plate is driven by the mechanical vibration of the LE-mode sub-resonators. The outer and inner transformers are used to address the electromechanical coupling from the

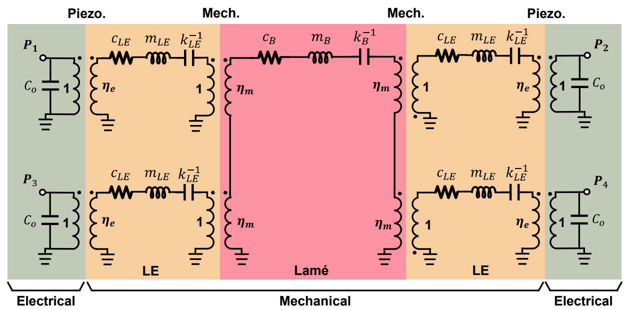

(a)

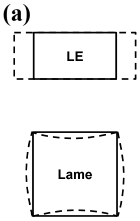

$f_{LE}=\frac{1}{2L_{LE}}\sqrt{\frac{1}{s_{11}\cdot\rho}}$	$k_{LE}=\omega_{LE}^2\cdot m_{LE}$	$C_o=\epsilon_{33}^S\frac{W_{LE}L_{LE}}{h}$
$m_{LE}=\frac{\rho W_{LE}hL_{LE}}{2}$	$c_{LE}=\frac{\sqrt{k_{LE}\cdot m_{LE}}}{Q}$	$k_t^2\approx\frac{\pi^2}{8}\frac{\eta_e^2}{k_{LE}\cdot C_o}$
$f_B=\frac{1}{\sqrt{2}L_B}\sqrt{\frac{C_{44}}{\rho}}$	$k_B=\omega_B^2\cdot m_B$	$\eta_e=2\cdot(e_{31,f}\cdot W_{LE})$
$m_B=\frac{\rho h L_B^2}{2}$	$c_B=\frac{\sqrt{k_B\cdot m_B}}{Q}$	$e_{31,f}=d_{31}/(s_{11}+s_{12})$

(b)

Figure 2: (a) Equivalent circuit model of the proposed support transducer resonator including electromechanical and mechanical coupling. (b) Formulas used to predict the resonant frequency, effective mass, damping, stiffness constant, and coupling factor for LE mode and Lamé mode resonators.

piezoelectric transducer in the LE-mode resonator and the mechanical coupling between different resonators respectively. Fig. 2(b) shows the equations used to calculate the parameters in the proposed analytical model.

For both LE-mode resonator and Lamé mode resonator, the effective mass, damping, and spring constant are derived from Rayleigh method with the mode shape equations. The effective mass for LE-mode (m_{LE}) could be derived by eq. (1) [13]

$$m_{LE}=\frac{\rho W\iint_A [u(x,z)]^2dxdz}{u_{max}^2}\approx\frac{\rho L_{LE}W_{LE}h}{2} \tag{1}$$

where ρ is the density, h is the thickness, L_{LE} is the length, and W_{LE} is the width of the LE-mode resonator, respectively. $u(x,z)$ and u_{max} are the mode shape equation and the maximum displacement of the length extensional mode resonator, respectively [14]. Note that the approximation for eq. (1) is set with the ideal boundary condition which the lateral dimension is much larger than the thickness dimension, e.g., $L_{LE}\gg h$. The effective mass for the Lamé mode (m_B) resonator is also derive with the similar topology. Eq. (2) express the calculation of the m_B [15]

$$m_B=\frac{\rho h\iint_A [w(x,y)]^2dxdy}{w_{max}^2}\approx\frac{\rho L_B^2 h}{2} \tag{2}$$

where L_B is the side length of the Lamé mode resonator. $w(x,y)$ and w_{max} are the mode shape equation and the maximum displacement of the Lamé mode resonator, respectively. The effective stiffness and damping constant for both resonators could be derived from the classic second order system as shown in eq. (3) and eq. (4)

$$k_{eff}=\omega_o^2\cdot m_{eff} \tag{3}$$

Table 1. Parameters used in the proposed model, including device dimensions, thickness configuration, material properties, and modeling parameters.

Device Parameters			**Thickness Configuration**		
LE		Lamé	SCS	AlN	Al
L_{LE}	W_{LE}	L_B	$10\ \mu m$	$0.5\ \mu m$	$1\ \mu m$
$214\ \mu m$	$60\ \mu m$	$200\ \mu m$			
Material Properties					
AlN					
ρ, density	C_{11}^E	C_{12}^E	C_{13}^E	C_{33}^E	ϵ_{33}^S
$3300\ kg/m^3$	$410\ GPa$	$149\ GPa$	$99\ GPa$	$389 GPa$	$9\cdot\epsilon_0\ F/m$
SCS					
ρ, density	C_{11}^E	C_{12}^E	C_{13}^E	C_{33}^E	C_{44}^E
$2330\ kg/m^3$	$195\ GPa$	$35\ GPa$	$64\ GPa$	$166\ GPa$	$80\ GPa$
Modeling Parameters					
LE					
c_{LE}	m_{LE}	k_{LE}	C_0	η_e	
$3.458\ \mu N\cdot s/m$	$1.73\times10^{-10}kg$	$3.164\ MN/m$	1.02 pf	$20.59\ \mu C/m$	
Lame					
c_B	m_B	k_B	η_m		
$9.431\ \mu N\cdot s/m$	$4.84\times10^{-10}kg$	$8.628\ MN/m$	1		

$$c_{eff}=\frac{\sqrt{k_{eff}\cdot m_{eff}}}{Q} \tag{4}$$

where k_{eff} is the effective stiffness constant, ω_o is the resonant frequency, m_{eff} is the effective mass constant, c_{eff} is the effective damping constant, and Q is the quality factor.

Electromechanical (η_e) and mechanical coupling (η_m)

Electromechanical coupling which enables by the piezoelectric effect could also be express by the numerical calculation. LE-mode piezoelectric resonator is actuated by the vertical electric field and induced the motion at the lateral dimension. This effect is coming from the piezoelectric coefficient (i.e., e_{31}) which represent the coupling between electric field and strain. The electromechanical conversion factor (η_e) is highly depends on the piezoelectric coefficient of the thin-film and the active area which electrode are covered. Eq. (5) shows the numerical expression of η_e

$$\eta_e=2\cdot(e_{31,f}\cdot W_{LE}) \tag{5}$$

where $e_{31,f}$ is the transverse piezoelectric coefficient [16], and W_{LE} is the width of the LE-mode resonator. Unlike previous work where the η_e is based on 1-D approach without considering the effect of the material Poisson's ratio [17], plane stress condition is considered in this work to compensate the error from the Poisson's ratio. Eq. (6) shows the calculation of $e_{31,f}$

$$e_{31,f}=\frac{d_{31}}{s_{11}+s_{22}} \tag{6}$$

where d_{31} is the piezoelectric coefficient in strain form, s_{11} and s_{22} are the compliance of the material.

Mechanical coupling (η_m) expresses the energy transfer from the LE-mode resonators to the Lamé mode resonator, which reveals the main idea of the support transducer topology. By connecting LE-mode resonators and a Lamé mode resonator at their maximum velocity location as shown in Fig. 1(a), this ensures almost 100%

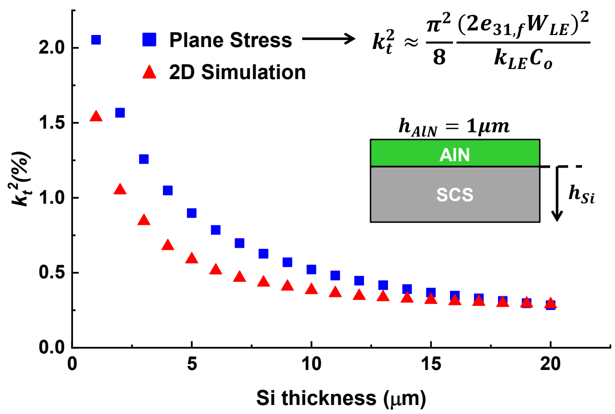

Figure 3: Comparison of the effective electromechanical coupling factor (k_t^2) with fixed h_{AlN} but varied h_{Si} based on plane stress and 2D FEM approach.

energy transfer among constituent resonant tanks. Thus, η_m in this case will be set as value 1 in the model representing no leakage during the energy transfer between resonators. For other devices using the same topology, they might not feature ~100% energy transfer due to the connection points between the transducer arms and the central bulk mode without ideal matching locations.

Table. 1 shows the device dimensions, thickness configuration, material properties, and the modeling parameters used in the analytical modeling. The length and width of the LE-mode resonators are 240μm and 60μm, respectively. The side length of the Lamé mode resonator is 200μm. The device was fabricated with the thickness configuration of 1μm aluminum (Al) serving as electrodes, 0.5μm aluminum nitride (AlN) piezoelectric thin-film, and 10μm Si device layer.

Implementation of Finite Element Method

Despite the electromechanical coupling factor (η_e) considering the Poisson's ratio in the previous section, we found that the numerical calculation based on plane stress condition still has a large error as compared to the FEM result. The error mainly comes from the unwanted out of plane displacement caused by the mismatch of the elastic modulus between the device layer (SCS) and AlN thin film. Previous work has demonstrated the compensation for this non-ideal effect by introducing multiple correction terms into the general equations with the help of FEM [18]. In this work, a 2D FEM simulations are performed to simultaneously correct the error and simplify the compensation process. Fig. 3 shows the comparison of the effective electromechanical conversion factor (k_t^2) with a fixed 1μm AlN thin film but varied thickness of SCS device layer from 1 - 20μm based on the plane stress condition and the FEM approach. The result discloses that a thinner silicon device layer deviates more on the k_t^2 of the piezoelectric contour mode resonator with fixed thickness of AlN thin film. This indicates that the numerical solution for the in-plane mode shape under TPoS configuration might also encounter the same problem.

EXPERIMENTAL RESULT

The proposed support transducer Lamé mode resonator is operated under differential driving and sensing scheme (DIDO) for the practical measurement, the FEM simulation, and the proposed analytical modeling. Fig. 4 shows the comparison of the frequency response between the proposed analytical modeling and the FEM simulation result with a given Q of 6,000. The magnitude and phase response from the equivalent circuit is in good agreement with the

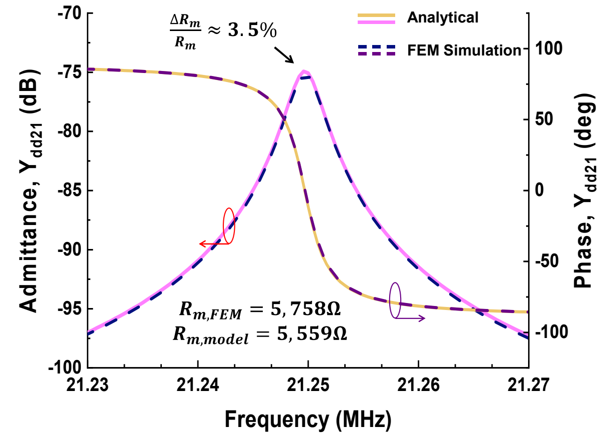

Figure 4: Frequency response from the proposed analytical model and FEM simulation under DIDO condition with a 3.5% error on the prediction of motional resistance.

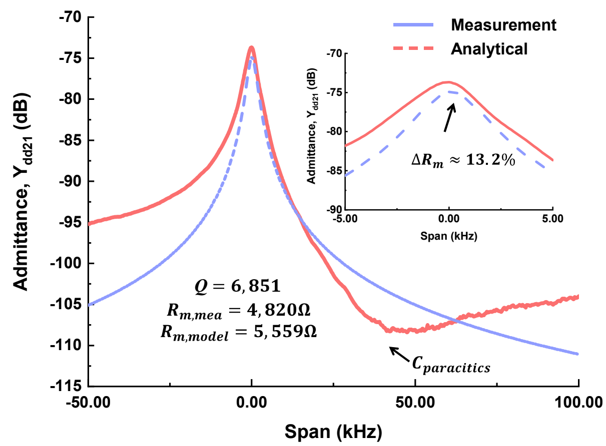

Figure 5: Frequency response of the measurement result and the proposed analytical model showing a 13.2% error on the motional resistance prediction.

FEM results. The motional resistance (R_m) from FEM and analytical model are 5,758Ω and 5,559Ω, respectively. A small difference on R_m of only 3.5% is observed, which confirms the accuracy of the proposed model. These results verify that the proposed analytical modeling can save significant computation time from the FEM in terms of the prediction of the frequency response and motional impedance of the support transducer resonator.

To complete this study, the frequency response of the fabricated device was measured using the network analyzer (Keysight E5071C) with virtual balun to enable DIDO configuration. Fig. 5 shows the comparison of frequency response between the measured admittance and the proposed analytical modeling using the measured Q-factor, 6,851. The Rm from measurement and analytical model are 4,820Ω and 5,559Ω, respectively. A 13.2% on the R_m prediction has been observed from the measurement result. In addition to the error of the motional impedance prediction, the frequency response is not in good agreement between measurement and the modeling.

The discrepancy between the modeling and the measurement might be attributed to the uncertainty in material properties, the asymmetry of the fabricated device, and parasitic capacitance from the experimental setup. For the device design with support transducer topology, there might be certain shift on the resonant frequency due to the variance from the fabrication process resulting in mismatch on each transducer arm. These frequency mismatches would lead to the leakage during the energy transfer between each sub-system and make the DIDO driving condition not fully cancel out the common mode noise.

CONCLUSION

In this work, an analytical model of the coupled piezoelectric resonator based on support transducer topology has been demonstrated with the comparison among analytical solutions, FEM results, and measurement data. With the help of FEM on the compensation of electromechanical coupling coefficient, the prediction of the motional impedance would only have 3.5% and 13.2% differences as compared to FEM and measurement, respectively. The proposed model can be extended to a reconfigurable mechanism on the analysis of the energy transfer in the coupled resonator system with different bulk mode configurations [19][20].

ACKNOWLEDGEMENTS

This work was supported by MOST 110-2622-E-007-022.

REFERENCES

[1] H. Lee *et al.*, "Low jitter and temperature stable MEMS oscillators," *Proc. IEEE Int. Freq. Control Symp.* (FCS), Baltimore, MD, USA, May 2012.

[2] D. B. Leeson, "A simple model of feedback oscillator noise spectrum," *Proc. IEEE*, vol. 54, no. 2, pp. 329–330, Feb. 1966.

[3] E. Rubiola, The Lesson Effect—Phase Noise in Quasilinear Oscillators. Cambridge, U.K.: Cambridge Univ. Press, Nov. 2008.

[4] A. Hajimiri *et al.*, "A general theory of phase noise in electrical oscillators," *IEEE J. Solid-State Circuits*, vol. 33, no. 2, pp. 179–194, Feb. 1998.

[5] Y.-W. Lin *et al.*, "Low phase noise array-composite micromechanical wine-glass disk oscillator," *Technical Digest, IEEE Int. Electron Devices Mtg.*, Washington, DC, Dec. 5-7, 2005, pp. 287-290.

[6] M.-H. Li *et al.*, "Optimizing the close-to-carrier phase noise of monolithic CMOS-MEMS oscillators using bias-dependent nonlinearity," *Technical Digest, IEEE Int. Electron Devices Mtg.*, San Francisco, CA, USA, Dec. 2014, pp. 22.3.1-22.3.4.

[7] G. Pillai *et al.*, "Exploration and Realization of Novel High-*Q* Bulk Modes Using Support Transducer Topology," *J. Microelectromech. Syst.*, vol. 30, no. 5, pp. 696-702, Jul. 2021.

[8] G. Pillai *et al.*, "Quality factor boosting of Bulk acoustic wave resonator based on a two dimensional array of high *Q* resonant tanks," *Appl. Phys. Lett.*, vol. 116, no. 16, pp. 163502, Apr. 2020.

[9] G. Pillai *et al.*, "Piezoelectric based support transducer design to enable high performance bulk mode resonators," *J. Microelectromech. Syst.*, vol. 28, no. 1, pp. 4-13, Nov. 2018.

[10] H.-T. Jen *et al.*, "High-*Q* support transducer MEMS resonators enabled low phase noise oscillators," *IEEE Trans. Ultrason., Ferroelectr., Freq. Control*, vol. 68, no. 4, pp. 1387-1398, Apr. 2021.

[11] G. Piazza *et al.*, "Piezoelectric aluminum nitride vibrating contour-mode MEMS resonators," *J. Microelectromech. Syst.*, vol. 15, no. 6, pp. 1406-1418, Dec. 2006.

[12] R. Abdolvand *et al.*, "Thin-film piezoelectric-on-silicon resonators for high-frequency reference oscillator applications," *IEEE Trans. Ultrason., Ferroelectr., Freq. Control*, vol. 55, no. 12, pp. 2596-2606, Dec. 2008.

[13] R. Holand, "Contour extensional resonant properties of rectangular piezoelectric plates," *IEEE Trans. Sonics Ultrason.*, vol. 15, no. 2, pp 97-104, Apr. 1968.

[14] G.K. Ho *et al.*, "Piezoelectric-on-Silicon Lateral Bulk Acoustic Wave Micromechanical Resonators," *J. Microelectromech. Syst.*, vol. 17, no. 2, pp. 512-520, Apr. 2008.

[15] J.E.-Y. Lee *et al.*, "Low loss HF band SOI wine glass bulk mode capacitive square-plate resonator," *J. Micromech. Microeng.*, vol. 19, no. 7, pp. 074003, Jun. 2009.

[16] S. Trolier-McKinstry *et al.*, "Thin Film Piezoelectrics for MEMS," *J. Electroceramics*, vol. 12, no. 1, pp. 7-17, Jan. 2004.

[17] V. Kaajakari, *Practical MEMS*, Las Vegas, Small Gear Publishing, 2009, pp. 307-324

[18] T. Cheng *et al.*, "A semi-analytical modeling approach for laterally-vibrating thin-film piezoelectric-on-silicon micromechanical resonators," *J. Micromech. Microeng.*, vol. 25, Oct. 2015.

[19] N. M. Nguyen *et al.*, "Design of piezoelectric MEMS bulk acoustic wave mode-matched gyroscopes based on support transducer," in *Proc. IEEE 34th Int. Conf. Micro Electro Mech. Syst.* (MEMS), Jan. 2021, pp. 338-341.

[20] C.-Y. Chang *et al.*, "Phase Noise Optimization of Piezoelectric Bulk Mode MEMS Oscillators Based on Phase Feedback in Secondary Loop," in *Proc. IEEE 35th Int. Conf. Micro Electro Mech. Syst.* (MEMS), Jan. 2022, pp. 212-215.

CONTACT

*S.-S. Li, tel: +886-3-516-2401; ssli@mx.nthu.edu.tw